Title
Modelling the soil-plant-atmosphere continuum in a Quercus-acer stand at Harvard forest: The regulation of stomatal conductance by light, nitrogen and soil/plant hydraulic properties

Journal
Plant, Cell and Environment, 19(8)

ISSN
0140-7791

Authors
Williams, M
Rastetter, EB
Fernandes, DN
et al.

Publication Date
1996

DOI
10.1111/j.1365-3040.1996.tb00456.x

Plant, Cell and Environment (1996) **19**, 911–927

THEORETICAL PAPER

Modelling the soil–plant–atmosphere continuum in a *Quercus–Acer* stand at Harvard Forest: the regulation of stomatal conductance by light, nitrogen and soil/plant hydraulic properties

M. WILLIAMS,[1] E. B. RASTETTER,[1] D. N. FERNANDES,[1] M. L. GOULDEN,[2] S. C. WOFSY,[2] G. R. SHAVER,[1] J. M. MELILLO,[1] J. W. MUNGER,[2] S.-M. FAN[2] & K. J. NADELHOFFER[1]

[1]*The Ecosystems Center, Marine Biological Laboratory, Woods Hole, MA 02543, USA, and* [2]*Division of Applied Sciences and Department of Earth and Planetary Sciences, Harvard University, Cambridge, MA 02138, USA*

ABSTRACT

Our objective is to describe a multi-layer model of C_3-canopy processes that effectively simulates hourly CO_2 and latent energy (*LE*) fluxes in a mixed deciduous *Quercus–Acer* (oak–maple) stand in central Massachusetts, USA. The key hypothesis governing the biological component of the model is that stomatal conductance (g_s) is varied so that daily carbon uptake per unit of foliar nitrogen is maximized within the limitations of canopy water availability. The hydraulic system is modelled as an analogue to simple electrical circuits in parallel, including a separate soil hydraulic resistance, plant resistance and plant capacitance for each canopy layer. Stomatal opening is initially controlled to conserve plant water stores and delay the onset of water stress. Stomatal closure at a threshold minimum leaf water potential prevents xylem cavitation and controls the maximum rate of water flux through the hydraulic system. We show a strong correlation between predicted hourly CO_2 exchange rate ($r^2 = 0{\cdot}86$) and *LE* ($r^2 = 0{\cdot}87$) with independent whole-forest measurements made by the eddy correlation method during the summer of 1992. Our theoretical derivation shows that observed relationships between CO_2 assimilation and *LE* flux can be explained on the basis of stomatal behaviour optimizing carbon gain, and provides an explicit link between canopy structure, soil properties, atmospheric conditions and stomatal conductance.

Key-words: *Quercus rubra*; *Acer rubrum*; soil–plant–atmosphere continuum model; photosynthesis; plant hydraulic conductance; stomatal conductance.

INTRODUCTION

Eco-physiological processes, such as photosynthesis and leaf energy balance, are now relatively well understood (McMurtrie 1993). What remains elusive is a sound understanding of how these processes integrate over space and time, and interact within a community of plants. Interest in scaling canopy processes derives in part from questions raised about the global carbon (C) cycle, and the nature of the missing terrestrial C sink (Schimel 1995). One approach to this problem uses models that allow scaling of processes at the leaf level to whole canopies (Jarvis *et al.* 1985; Running & Coughlan 1988; McMurtrie 1993). Such models closely predict hourly CO_2 flux measurements in temperate grasslands (Norman & Polley 1989), a soybean crop (Baldocchi 1992), and temperate forest (Amthor 1994), although the latter model tended to overestimate CO_2 uptake in the afternoon (Amthor *et al.* 1994). Our goal in this paper is to describe a process-based model that accurately predicts whole-forest carbon and water exchange, and explains these fluxes in terms of optimal water and nitrogen (N) use. Such a model both improves our understanding of key factors in forest growth and ecosystem function, and provides a synthetic tool with which to investigate the behaviour of canopies at different sites.

Both aggregated (e.g. 'big-leaf') and distributed (e.g. multi-layer) approaches are commonly applied in modelling canopy processes (Raupach & Finnigan 1988). There are costs and benefits to both (O'Neill & Rust 1979; Rastetter *et al.* 1992). Distributed simulations require assumptions about the distribution of key parameters in space, but allow model parametrization using fine-scale (e.g. leaf-level) data. Aggregation avoids the need for spatial details by building the effects of non-linearities into the model parameters; however, fine-scale data are not directly applicable to estimation of these coarse-scale parameters. These parameters must therefore be estimated directly from coarse-scale data (e.g. canopy rather than leaf-level data).

Big-leaf modelling is an aggregated approach commonly applied in simulations of canopy processes (Sinclair *et al.* 1976); photosynthetic properties of individual leaves are assumed to be scaled with depth in the canopy in rela-

Correspondence: Mathew Williams, The Ecosystems Center, Marine Biological Laboratory, Woods Hole, MA 02543, USA.

tion to photosynthetic photon flux density (PPFD) profiles (Farquhar 1989; Field 1991). If this is so, then details of the canopy profile can be ignored in many cases, and the modelling approach can be simplified to treat only a single layer. However, if the interaction between microclimate and physiology is of interest, then it is important to resolve detail within the canopy using a distributed approach (Raupach & Finnigan 1988). The model we present is based in part on a hypothesized spatial independence of stomatal control, and therefore precludes an aggregated approach. Atmospheric saturation deficit, net radiation and leaf boundary layer conductance all vary with depth in the canopy; also, the rate of water supply may depend on the height of the leaves above the ground. This means we expect vertical variation in patterns of water stress, and thus the degree of stomatal limitation may vary with height in the canopy. To investigate and account for this phenomenon, we employ a 10-layer canopy model.

Our model is a new synthesis, combining simple models of plant and soil hydraulics, carbon assimilation, gas diffusion and vegetation/environment interactions to produce a robust model of the soil–plant–atmosphere continuum. The model is unique in that g_s for each layer is calculated to maximize daily C gain per unit leaf N, within the limitations of canopy water storage and soil-to-canopy water transport. Transpiration is ultimately limited by the rate of water supply imposed by plant hydraulics (Tyree 1988) and soil water availability (Gollan *et al.* 1985).

Cowan (1977) has proposed a mechanism of optimal stomatal variation that regulates the relationship between water loss and carbon gain. We employ a similar mechanism that operates to ensure the efficient use of canopy *stored water* so it can be more optimally employed ameliorating afternoon water stress. Once stored water is exhausted, leaves must be irrigated by water transported from the soil (Meinzer & Grantz 1990); g_s adjusts so that transpiration equals the rate of water supply (Aston & Lawlor 1979). The maximum rate of water supply is determined by the minimum sustainable leaf water potential, canopy capacitance, root water uptake, soil water availability, and stem hydraulic conductance (Meinzer & Grantz 1991). Stomatal closure at a threshold minimum leaf water potential prevents xylem cavitation and controls the maximum rate of water flux through the hydraulic system (Jones 1992).

We parametrize and drive the model with meteorological data and measurements of vegetation structure collected at Harvard Forest, Petersham, MA (42°54′N, 72°18′W, elevation, 340 m) during the summer of 1992. The model then predicts the CO_2 exchange rate and transpiration rate of each canopy layer; from measurements of other fluxes within the system (e.g. soil respiration and evaporation), we can predict the diurnal course of whole-forest fluxes. The eddy correlation method (Baldocchi *et al.* 1988) has provided independent measurements of the hourly fluxes of carbon and latent energy from the forest canopy for entire growing seasons at Harvard Forest (Wofsy *et al.* 1993). We compare the simulated and measured diurnal fluxes of CO_2 and latent energy (LE), and discuss the influence of plant hydraulics on flows. We use sensitivity analysis to determine the most influential set of parameters, and discuss future directions for model development and application.

MODEL STRUCTURE

The model (Fig. 1) consists of various sub-models, which can be roughly divided into physical and biological components. The physical components specify the structure of the canopy, determine the absorption of both photosynthetically active radiation (PAR) and other wavelengths in each canopy layer, calculate leaf boundary layer conductance, and determine soil water availability. The biological components determine how leaf water potential varies with transpiration, the variation of leaf biochemical parameters with foliar N content, irradiance and leaf temperature, and the diurnal course of g_s in each layer, which controls C uptake and water loss.

Physical sub-models

The physical sub-models are calculated only once per time step (30 min). Hourly meteorological data collected at Harvard Forest were linearly interpolated to estimate conditions on the half-hour. In the physical components we have four sub-models as follows.

(A) Canopy structure

The canopy is divided into 10 layers, with equal leaf area per layer, spaced equally between the top (24 m) and bottom (10·5 m) of the canopy. Ellsworth & Reich (1993) and Aber (1979) have shown that such a leaf area distribution is a reasonable assumption in closed deciduous forests. We analysed data from Ellsworth & Reich (1993) showing the variation in N concentration (g m^{-2} *leaf area*) with height in a deciduous forest, and fitted an exponential decay function that effectively described this relationship (see Eqn A1). We used this function to allocate the total canopy N measured at the site among the 10 canopy layers.

(B) Radiation regime

The radiation routines model the incidence, interception, absorption and reflection of PAR, near infrared radiation (NIR), and longwave radiation. PPFD (μmol m^{-2} s^{-1}) was measured at the Harvard Forest site; from the integrated daily total, we estimated the diffuse fraction of the incoming flux (Erbs *et al.* 1982). Using relationships from Szeicz (1974), we approximate the incidence of NIR (i.e. the remaining component of the shortwave radiation) in W m^{-2}.

To determine solar radiation absorption, we employ Beer's Law as described in Amthor (1994) and Amthor *et al.* (1994). Their multilayer model of radiation absorption by the canopy accounts for individual leaf and forest floor

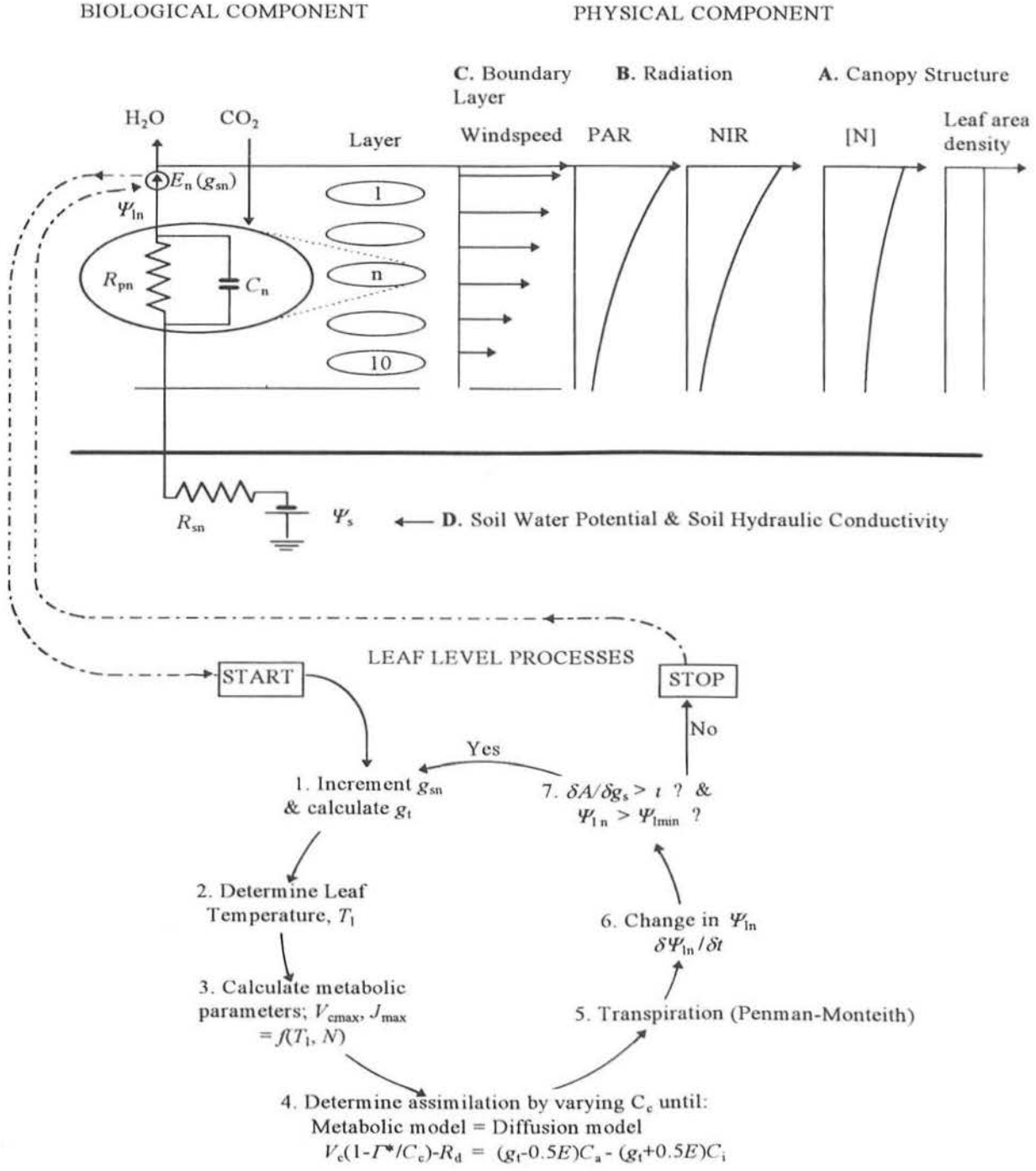

Figure 1. The canopy model is divided into physical and biological components. The former have four facets, consecutively calculated as lettered in the diagram, relating to (A) the variation in leaf area density and leaf nitrogen content ([N]) with depth in canopy (the vertical axis); (B) the vertical distribution of radiation – PAR, NIR and longwave (not shown); (C) the distribution of wind speed and leaf boundary layer conductance within the canopy, and (D) the soil water potential (Ψ_s) and soil hydraulic conductivity. The biological component is then applied successively to each canopy layer. Biological processes are calculated iteratively by incrementing layer stomatal conductance (g_{sn}) until this results in either no appreciable increase in assimilation (defined by a parameter ι), or the minimum leaf water potential (Ψ_{lmin}) has been reached. The iterative procedure is calculated as follows: (1) g_{sn} is incremented and total conductance to CO_2 (g_t) is calculated; (2) the leaf energy balance and thus leaf temperature (T_l) are estimated; (3) the Rubisco-limited rate of carboxylation (V_{cmax}) and the potential rate of electron transport (J_{max}) are determined from T_l, irradiance and leaf N content; (4) mesophyll CO_2 concentration (C_c), and thus CO_2 assimilation are calculated: as g_{sn} increases, assimilation becomes less limited by diffusion (V_c is the actual rate of carboxylation, and Γ^* is the CO_2 compensation point); (5) g_{sn} also drives layer transpiration (E_n), determined by the Penman–Monteith equation; (6) each layer has an independent hydraulic system (illustrated for layer n, where R_{pn} is layer plant resistance, C_n is layer capacitance and R_{sn} is soil hydraulic resistance to this layer), which determines the lagged change in leaf water potential (Ψ_{ln}) caused by transpiration. The cycle of increases in g_{sn} is terminated when either one of the conditions in (7) is no longer met (N.B. ι is small).

reflectance and absorptance of NIR, PAR and longwave radiation. Reflectivity and transmissivity of leaves and soils were estimated from data provided by Baldocchi *et al.* (1985). We assumed a spherical leaf angle distribution (Russell *et al.* 1989). The sum of PAR (derived from PPFD), NIR and longwave radiation absorbed determines the net isothermal radiation for each canopy layer.

(C) Leaf boundary layer characteristics

The multilayer approach requires that we estimate the variation of boundary layer characteristics of leaves within the canopy. Measurements were made at the Harvard Forest tower of wind speed (m s^{-1}) and direction (°) at 30 m, 6 m above the canopy surface. However, wind speeds, and thus boundary layer conductances, decline within the canopy (Roberts *et al.* 1990). We use an exponential wind relationship (Cionco 1985) to approximate the wind speed at different heights within the canopy. Within each canopy layer, we estimate the leaf boundary layer conductances to water vapour and heat using relationships from Nobel (1983). At Harvard Forest, measured midday CO_2 concentrations at 30 m (6 m above the canopy) and within the canopy vary by less than 1 μmol mol^{-1}. On this evidence, we will assume that conductance across the canopy boundary layer is high enough to be ignored.

(C) Soil water characteristics

Soil water potential (Ψ_s) and soil hydraulic conductivity (L_{soil}) were not measured directly, but can be estimated from soil sand, clay and water content using empirical relationships (Saxton *et al.* 1986). Evaporation of water from the soil surface is determined from soil radiation balance (calculated in the radiation regime) and soil water content (Amthor *et al.* 1994). Soil moisture levels are high around the study site at Harvard Forest (see below), so we expect soil water to be freely available throughout the growing season in this case.

Biological sub-models

The key hypothesis governing the biological components of the model is that g_s is controlled to maximize carbon gain per unit N within the limits set by the rate of water uptake and canopy water storage. Studies on *Quercus rubra* (Ren & Sucoff 1995) and other species (Kuppers 1984; Meinzer & Grantz 1990) have shown a coordination of vapour-phase and liquid-phase conductances. Meinzer & Grantz (1991) hypothesize that g_s will ideally remain in balance with the hydraulic capacity of the soil and roots to supply the leaves with water, avoiding leaf desiccation at one extreme and the unnecessary restriction of CO_2 uptake at the other. We model this explicitly, and also include the impacts of water stored by plants.

Component plants are assumed to open their stomata until either (1) further opening does not constitute an effective use of stored water in terms of carbon gain per unit water loss, or (2) further opening causes a drop in leaf water potential below the limit that causes xylem cavitation. Plant water relations are modelled as an analogue to a simple electrical circuit (Cowan 1965; Passioura 1982; Whitehead & Hinckley 1991). Each canopy layer is assumed to have an independent connection to soil water. Therefore, each layer is modelled separately.

Soil resistance

We use a single soil layer steady-state model (Newman 1969; Federer 1979) to estimate the hydraulic resistance of the soil around the roots that supply each canopy layer (R_{sn}; MPa s m^2 $mmol^{-1}$). The model is dependent on root dimensions and soil hydraulic conductivity (see Appendix). We assume that each canopy layer is supplied by an equal proportion of the total root length, and so R_{sn} is invariant among layers. The single soil layer is an appropriate approximation for Harvard Forest because of high moisture levels (see below), but a more detailed soil profile might be needed in dry soils.

Plant hydraulics

The highest layers in the canopy are subject to the greatest resistance to xylem water supply (Hellkvist *et al.* 1974). Thus, xylem hydraulic resistance per unit leaf area for layer n in the canopy (R_{pn}; MPa s m^2 $mmol^{-1}$) increases with the layer height (h). We make various simplifying assumptions in our representation of plant hydraulics. Analogous with a pipe model (Shinozaki *et al.* 1964), each layer is served by an independent water supply system. We employ an unbranched model, rather than a branched catena (Tyree 1988), because of its greater simplicity, and because we are representing a canopy of many individuals, rather than modelling a single tree. The whole canopy can be visualized as a set of 10 parallel circuits (only one of which is shown in Fig. 1). A separate branch hydraulic resistance is not specified, but is assumed to be included with the value of R_{pn}.

The water in the xylem can rupture under the extreme tensions that occur naturally – there is often a threshold water potential for such cavitation (Jones 1992). The onset of xylem cavitation can lead to a rapid and catastrophic decline in stem hydraulic conductivity by inducing further cavitations (Tyree & Sperry 1989). Jones & Sutherland (1991) have shown that the maintenance of a maximally efficient conducting system requires that stomata close as evaporative demand rises to prevent shoot water potentials falling below this threshold value (Ψ_{lmin}). Tyree & Dixon (1986) have measured the threshold value for *Acer saccharum* as –2·5 to –3·0 MPa. Bassow (1995) reports that measured leaf water potentials of *Q. rubra* near the Harvard Forest site do not fall below –2·5 MPa; this value is used in modelling the threshold.

Dynamic flow

The relationship between the flux of water through the

plant and the water potential drop is not unique; initially water is drawn from stores within plant tissues, so that liquid flow lags the transpirative demand (Landsberg *et al.* 1976; Schulze *et al.* 1985). This hysteresis can be modelled by incorporating capacitors into the circuit analogue to represent canopy water storage capacity (Jones 1978).

Assuming constant capacitance (C_n), the change in leaf water potential of canopy layer n over a time step Δt can be described by

$$\Delta\Psi_{ln} = \Delta t \frac{\Psi_s - \rho_w g h - E_n(R_{sn} + R_{pn}) - \Psi_{ln}}{C_n(R_{sn} + R_{pn})}, \quad (1)$$

where ρ_w is the density of liquid water (kg m^{-3}), g is gravitational acceleration (9·8 m s^{-2}) and h is the height (m) of the canopy layer n (see Appendix for derivation). The response times of both crop plants (Jones 1978) and trees (Schulze *et al.* 1985) indicate that a time step of 30 min is adequate to resolve the dynamic behaviour using this equation.

Jones (1978) used a similar lumped-parameter model to simulate diurnal trends of Ψ_l in transpiring wheat, and found that it could account for more than 90% of the variation in hourly means of Ψ_l. However, we do not believe that this approach has been used to predict g_s, and thus determine the hypothetical water supply limitations to productivity.

Tyree & Sperry (1988) undertook hydraulic measurements for *Acer saccharum* in Vermont and estimated the hydraulic conductivity (G_p) to be 4·0 mmol s^{-1} m^{-1} MPa^{-1} ($R_{pn} = h/G_p$; see Appendix). The conductivity of *Quercus rubra* is of similar magnitude (Cochard & Tyree 1990). We assume that ring-porous *Quercus* will have a slightly higher conductivity than *Acer*, and so we use an estimate of 4·5 for model testing. This figure gives R_{pn} values close to those measured for larger *Q. rubra* seedlings (Ren & Sucoff 1995).

Schulze *et al.* (1985) have estimated total tree stored water usage for adult *Picea abies*. An individual *P. abies* used 16·2 kg of stored water in a day; needle biomass was 13·1 kg. Using leaf mass per unit area relationships for *P. abies* (Oren *et al.* 1986), we estimate the amount of stored water per unit leaf area as 8·8 mol m^{-2}. The drop in leaf water potential during stored water usage was 1·1 MPa, so we estimate capacitance (C_n) at 8·0 mol MPa^{-1} m^{-2}. Although C_n is expressed on a leaf area basis, the stored water is distributed in both foliage and the woody tissue of the crown. Landsberg *et al.* (1976) estimated the capacitance of potted apple trees to be similar, around 5·0 mol MPa^{-1} m^{-2}. The value of Schulze *et al.* (1985) is probably more applicable to this model because it was measured for full-sized canopy trees in the field. However, because of the uncertainty associated with this value, a sensitivity analysis has been performed on C_n (see below).

Leaf biochemical parameters

The model used to determine photosynthesis is described elsewhere (Farquhar & Von Caemmerer 1982), but the calculation of the parameters required is detailed below. Photosynthesis is limited by the minimum of the ribulose bisphosphate carboxylation rate and the rate of ribulose bisphosphate (RuBP) regeneration. The maximum rates of these two processes and their temperature and N dependences must be calculated.

Maximum carboxylation capacity (V_{cmax})

We assume that V_{cmax} is proportional to foliar N concentration (Harley *et al.* 1992), and can be described by the following relationship:

$$V_{cmax} = N k_{tc} \kappa_c, \quad (2)$$

where k_{tc} is a temperature coefficient (a temperature-dependent polynomial function normalized to 30°C; Kirshbaum & Farquhar 1984), and κ_c is a catalytic rate constant (μmol CO$_2$ g^{-1} N s^{-1}). κ_c is calculated from measured values of N and V_{cmax}. The maximum leaf N contents at Harvard Forest in 1992 were 3·6 g m^{-2} leaf area for *Q. rubra* and 2·3 g m^{-2} for *A. rubrum* (Bassow 1995). To match these values, we selected the highest values of V_{cmax} recorded for these or similar species in the literature; around 51 μmol CO$_2$ m^{-2} *leaf* s^{-1} for *Q. rubra*, and around 31·6 μmol CO$_2$ m^{-2} leaf s^{-1} for *A.saccharum* at 30 °C (Wullschleger 1993) (the value for *A.saccharum* has been corrected from 25 °C). However, Epron *et al.* (1995) argue that these values are underestimates, because the data in Wullschleger (1993) are calculated based on the internal CO$_2$ concentration (C_i) rather than the concentration at the carboxylation site (C_c). In woody plants, C_c can be substantially lower than C_i because of low internal conductances (g_i). Our biochemical model has been modified to include g_i (see Eqn A11) as estimated by Epron *et al.* (1995), and the values of V_{cmax} have been corrected by a simple scaling to reflect this modification. The corrected values are 122 μmol CO$_2$ m^{-2} leaf s^{-1} for *Quercus*, and around 75 μmol CO$_2$ m^{-2} leaf s^{-1} for *Acer*. From the data provided, we obtain similar values of κ_c for both species: 33·9 for *Quercus* and 32·8 for *Acer*, giving a site average κ_c of 33·6 μmol CO$_2$ g^{-1} N s^{-1}.

Maximum electron transport rate (J_{max})

Harley *et al.* (1992) have also demonstrated that J_{max} values are proportional to foliar N concentration, justifying the following relationship:

$$J_{max} = N k_{tj} \kappa_j, \quad (3)$$

where k_{tj} is a temperature coefficient (of similar functional form to k_{tc}) and κ_j is the electron transport rate coefficient (μmol g^{-1} N s^{-1}) which we calculate from measured values of N and J_{max}. J_{max} values for *Q. rubra* have been determined from A/C_i curves (Loreto & Sharkey 1990) at 127 μmol m^{-2} leaf s^{-1}. However, Epron *et al.* (1995) show that J_{max} values are higher when calculated from A/C_c curves for woody species. We therefore correct the *Quercus* value to 165 μmol m^{-2} leaf s^{-1} at 30 °C. We

estimate J_{max} values for *Acer* by assuming that the V_{cmax}:J_{max} ratio is similar for both species; the estimated value is 94 μmol m^{-2} leaf s^{-1}. Using the maximum foliar N concentrations listed above, the site average κ_j is then calculated as 44·3 μmol g^{-1} N s^{-1}. We determine the potential rate of electron transport from J_{max} and absorbed PPFD (Farquhar & Wong 1984).

Biochemical parameters

Several other parameters are required for the photosynthesis model (Farquhar & Von Caemmerer 1982). The values and temperature dependences of K_c and K_o, the Michaelis–Menten constants for enzyme catalytic activity for CO_2 and O_2, respectively, are taken from Kirschbaum & Farquhar (1984) and McMurtrie *et al.* (1992). We derive Γ^*, the CO_2 compensation point in the absence of non-photorespiratory respiration, from measurements of V_{cmax}, amongst other parameters. Epron *et al.* (1995) suggest that observed values of Γ^* in woody plants are overestimated from A/C_i curves because internal resistance to CO_2 diffusion is unaccounted for. We account for this resistance (see below), and so we can approximate woody plant Γ^* by that of herbaceous plants, 36·5 μmol mol^{-1} at 25 °C (Epron *et al.* 1995), using an Arrhenius relationship for temperature sensitivity (McMurtrie *et al.* 1992). We determine the respiration rate of each layer (R_d; μmol m^{-2} s^{-1}) from foliar N content and leaf temperature, using relationships and parameters described by Ryan (1991).

Impacts of water status

Following Cornic *et al.* (1989), we assume that the photosynthetic apparatus is resistant to drought. Epron & Dreyer (1993) have shown that, in the leaves of young oak saplings (*Quercus petraea*) subjected to water stress, there was only a limited decline in maximum photosynthetic rates, and the photochemistry of photosystem II and the quantum yield of light-driven electron transport remained stable. We therefore assume that water stress affects only g_s, and not the photosynthetic mechanism.

Leaf level processes

For each canopy layer, once every 30 min an iterative procedure is used to determine the maximum stomatal conductance in this layer (g_{sn}) and the assimilation rate associated with this conductance (see Fig. 1).

The iterative procedure is as follows, starting from a very low g_s.

(1) Increment g_{sn} by a small amount (*c.* 1 mmol m^{-2} s^{-1}).
(2) Determine leaf temperature (T_l, °C) resulting from the leaf energy balance at this g_{sn} using a steady-state approximation (Jones 1992).
(3) Determine leaf biochemical parameters, based on foliar N concentrations (Field & Mooney 1986), absorbed PPFD and leaf temperature.
(4) Determine the equilibrium mesophyll CO_2 concentration (C_c) that satisfies both diffusion from the atmosphere to the mesophyll (see Appendix) and metabolic uptake, as described by Farquhar & Von Caemmerer (1982).
(5) Calculate layer transpiration rate (mmol m^{-2} s^{-1}) at this g_{sn} with the Penman–Monteith equation (Jones 1992).
(6) Calculate the change in layer leaf water potential (Ψ_{ln}) after one time step (Δt, 1800 s) of transpiration at the specified g_{sn}, using Eqn 1.
(7) Return to step 1 (for a further increment of g_{sn}), unless either:
(a) previous g_{sn} increment failed to raise assimilation appreciably (see below), or
(β) Ψ_{ln} has reached its specified cavitation limit (Ψ_{lmin}). The water supply system is now operating at its maximum rate; any further increase in g_{sn} would take the xylem beyond its threshold for cavitation, and result in a catastrophic failure in water supply.

It is this iterative procedure of setting g_s, especially as relates to step (7), that sets our canopy model apart from similar models. Embedded in this procedure is our underlying hypothesis that stomatal variation operates to minimize water stress, by effectively using stored water to maximize C gained per unit water loss over the course of a day, and by preventing xylem cavitation.

Figure 2 shows the response of net leaf layer CO_2 assimilation rate (A) and transpiration to g_s, in the topmost canopy layer at noon on a representative day (see Fig. 5, day 215, for prevailing environmental conditions – these are held constant through the iteration). After an initially rapid increase, the response of A becomes asymptotic, and the carbon gain per unit water loss declines. We argue that plants use their water store conservatively; it is more efficient to limit g_{sn} when atmospheric saturation deficits are low (morning), so that stored water can be utilized later to

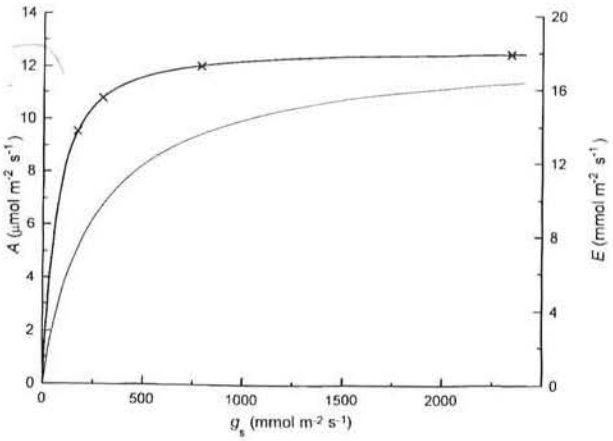

Figure 2. Typical upper canopy response of A, assimilation rate (——) and E, transpiration rate (——) to stomatal conductance. The crosses mark where t (stomatal threshold) is equal to 0·2, 0·07, 0·01 and 0·001% (reading from left to right).

buffer the impacts of high afternoon atmospheric saturation deficits. For this reason, optimal g_{sn} is fixed when an increment in g_{sn} (≈1 mmol m^{-2} s^{-1}) fails to increase A by more than 0·07% (the threshold parameter t). t was initially selected using Fig. 2, to give maximum conductances of 300 mmol m^{-2} s^{-1}, in accordance with measured maxima for *Q. rubra* (Weber & Gates 1990).

Site description

The model results were compared with hourly measurements of whole-canopy exchange made at Harvard Forest during the 1992 growing season (Wofsy *et al.* 1993; Goulden *et al.* 1996). The forest to the south-west of the tower is mainly composed of *Quercus rubra* L. (≈70% of the leaf area) and *Acer rubrum* L. (≈30% of the leaf area; Amthor *et al.* 1994). We focused on days with no more than one data point missing per day, and with winds predominantly from the south-west. We compared daytime flux predictions with measurements of *LE* (Wm^{-2}) and net ecosystem exchange of CO_2 (*NEE*). *NEE* (μmol m^{-2} s^{-1}) is the net of gross canopy CO_2 uptake (carboxylation and oxygenation) and leaf, soil and stem respiration. A negative *NEE* represents a net flux into the forest (i.e. assimilation exceeds respiration).

The experimental methods used at Harvard Forest, and the accuracy of the measurements, are described by Goulden *et al.* (1996). Individual hourly flux measurements are subject to random variability of order ± 20% because of the finite sampling period used (Baldocchi *et al.* 1988). This creates scatter in the comparison between predicted and measured fluxes that over time average to zero. Systematic errors during the day, which reflect a consistent discrepancy between the true flux and the measured flux (e.g. a calibration error), are no greater than 10–20% (Goulden *et al.* 1996).

Measurements showed that temperature (°C) and atmospheric saturation deficit (kPa) varied slightly between the top and bottom of the canopy; values for the middle layers were derived by interpolation. Incident PPFD (μmol m^{-2} s^{-1}) was measured at 30 m and used to calculate incident NIR. Ambient CO_2 concentration (μmol mol^{-1}) was measured at 30 m. Total leaf nitrogen was set at 6·7 g N m^{-2} ground area, based on the foliar nitrogen content reported for Harvard Forest by Aber *et al.* (1993), and LAI was set to 3·5, based on leaf litter collections made in the fall of 1992 near the eddy correlation tower (Amthor *et al.* 1994). The model assumes that LAI is equally distributed between 10 and 24 m (Aber 1979; Ellsworth & Reich 1993). We assume a mean fine root radius of 0·35 mm, and a fine root density (l_R) of 1300 m m^{-2}, using data collected at Harvard Forest by McClaugherty, Aber & Melillo (1982). The partitioning between soil and stem respiration was made following Goulden *et al.* (1996).

Soil moisture levels to the south-west of the tower are high. Soil pits dug up to 60 m south-west of the tower had standing water at 30 cm depth during the summer of 1994 (Rich Boone, Harvard Forest, personal communication). This section of forest seems to be well supplied with water throughout the growing season, so we assume that soils are at field capacity in model runs. Therefore, water limitations of canopy processes in these simulations are the result of restricted conductance through the soil–root–stem system, not the result of low soil moisture. Soil maps at Harvard Forest indicate that sandy loams lie south-west of the tower, with ≈60% sand content and 10% clay content.

RESULTS AND DISCUSSION

The model predicts diurnal variation in one parameter (g_s) in each canopy layer. In combination with environmental conditions, g_s determines the magnitude of canopy water and carbon fluxes. Modelled rates of soil evaporation are added to the transpiration rates of the canopy layers to give whole-forest *LE*. The net of individual layer CO_2 exchange rates and soil and stem respiration rates provides our estimate of *NEE*.

The model was tested against hourly flux measurements from 25 d with complete data sets and varying weather conditions from the summer of 1992 (Fig. 3). From regression analysis of measured versus predicted fluxes during daylight hours (n = 317), the r^2 values were 0·83 for *LE* (slope 0·85 ± 0·02) and 0·82 for *NEE* (slope 1·05 ± 0·02). The model tended to underpredict *LE* in some instances. The wind quadrant for each flux reading is indicated by the symbols in Fig. 3. Because the model was parametrized with data from the canopy south-west of the tower, we reanalysed the data for periods in which winds were solely from this direction (n = 139); the r^2 values were 0·87 for *LE* (slope 1·01±0·02) and 0·86 for *NEE* (slope 1·03±0·02). Thus, when winds are from the south-west the model makes more accurate predictions, and the slopes of the regression lines do not differ significantly from 1·0. The model underestimates *LE* when winds are from the north-west, an area with swampy conditions, and where key parameters like LAI may differ from those used in the model.

Predictions for four days between the end of July and early September, with winds consistently from the south-west, are examined in detail (Fig. 4). The only differences among the modelled days are the measured environmental conditions and calculated diurnal variation in solar elevation. The full set of parameters used in the model runs are shown in Table 1. In discussing model output, we show predictions at the whole-canopy level (Fig. 4) and also for individual canopy layers (Figs 6 & 10). Our model is designed to make predictions at the whole-forest level, and thus Fig.4 is used for quantitative model confirmation. In presenting data for the individual layers, the details of model behaviour are displayed. A degree of aggregation has been employed in parametrizing each canopy layer; a simple weighted average was applied to take account of species differences. Thus, we use the comparison of canopy layer level predictions with leaf level data purely as a qualitative confirmation of the model.

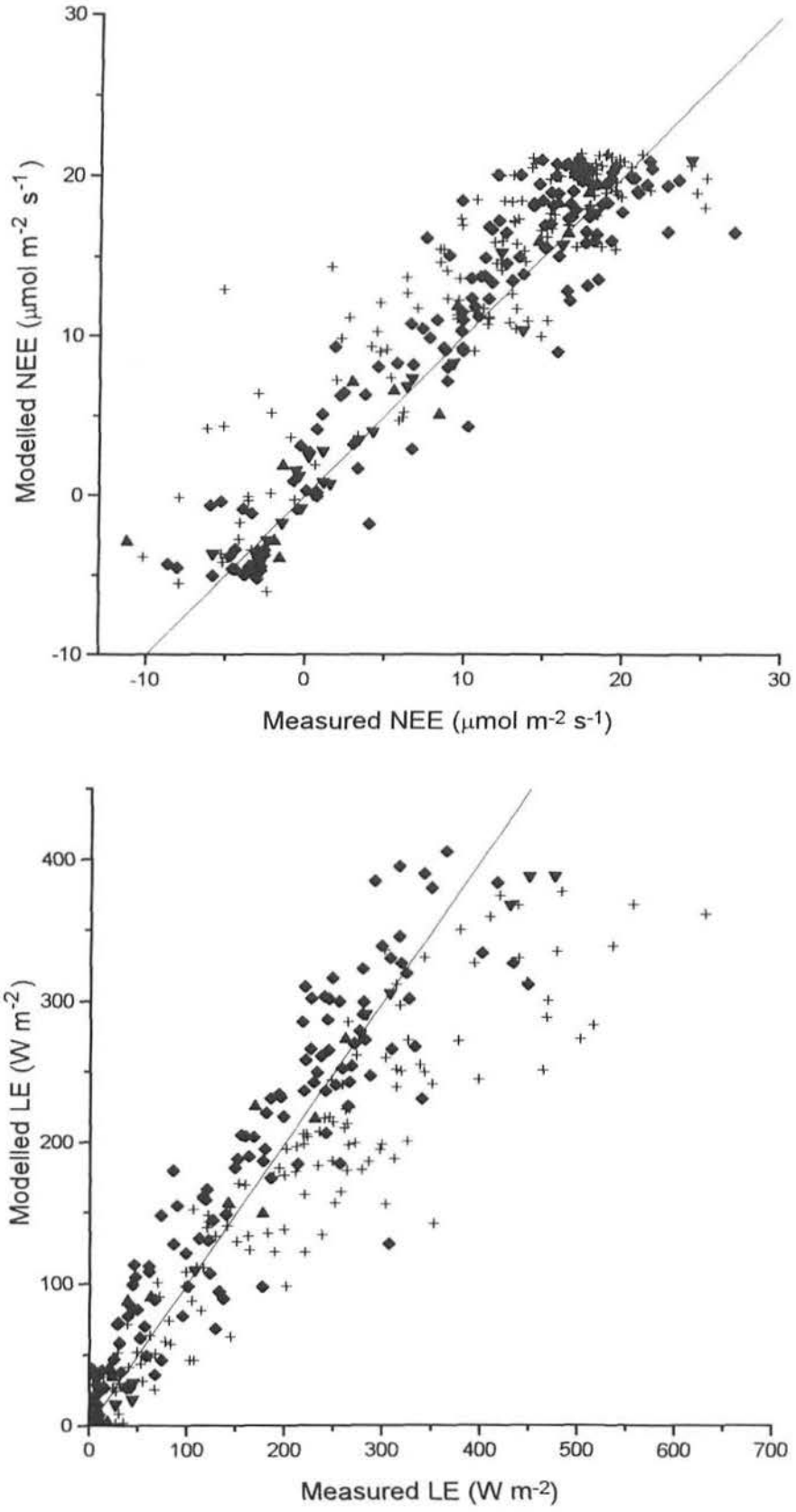

Figure 3. Modelled values of *NEE* (top) and *LE* (bottom) are plotted against their measured values for 25 d in the summer of 1992. The symbols indicate the wind quadrant at the time of the flux measurement: NE (▲), SE (▼), SW (◆) and NE (+). The 1:1 line is indicated on each graph.

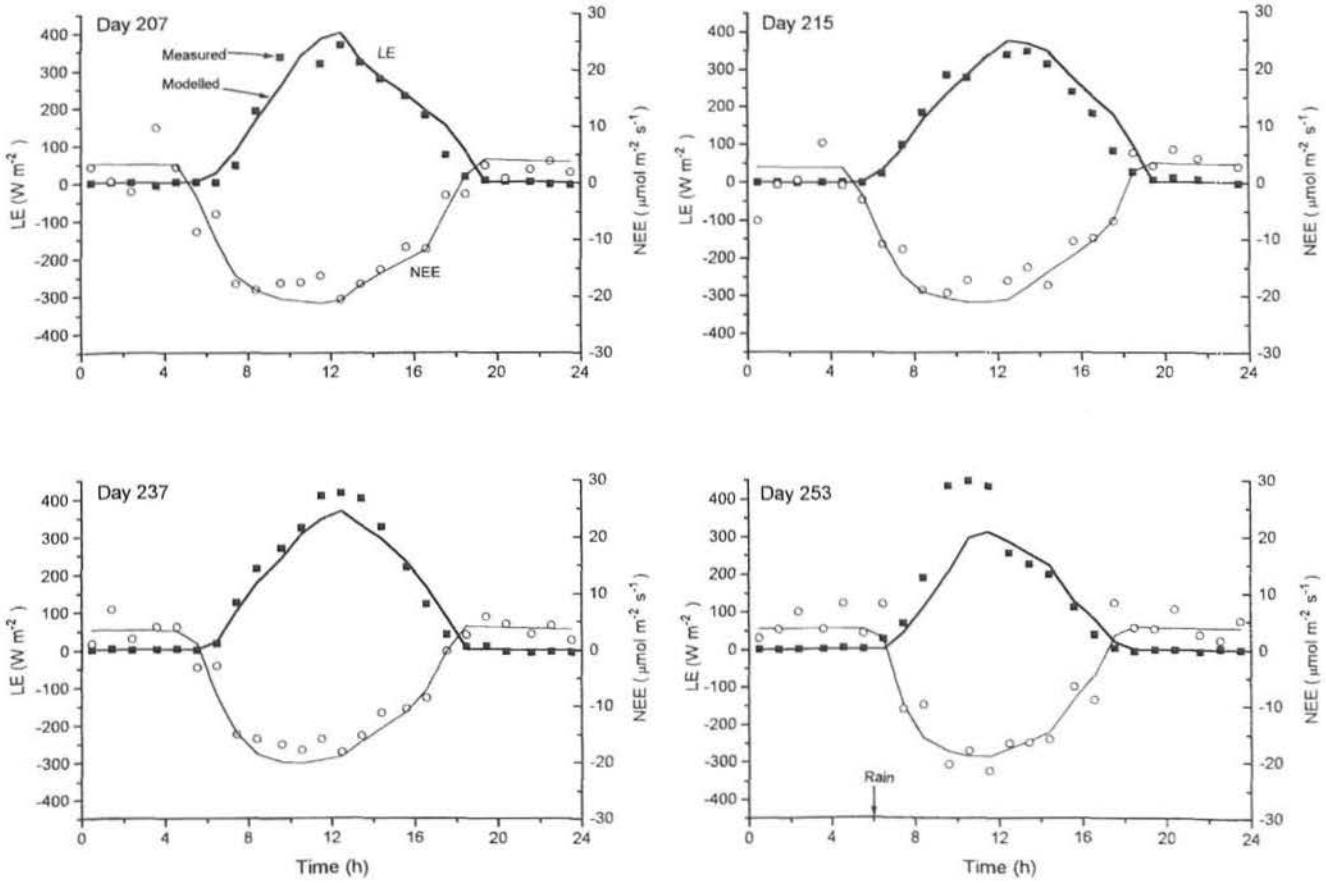

Figure 4. Diurnal course of predicted (lines) and measured (symbols) *Quercus–Acer* forest net ecosystem exchange (—— / ○) and latent energy (—— / ■) during four days in 1992 with nearly complete eddy correlation data and winds from the south-west.

Whole-forest hourly CO_2 exchange

During the course of the day, canopy processes are initially driven by the interception of incident radiation (Figs 4 & 5). As stomata open, CO_2 assimilation rises more rapidly than *LE*, because atmospheric saturation deficit is low in the cool of the morning (Fig. 5). With rising air temperatures, atmospheric demand for water, and thus transpiration, are increased. As light becomes saturating, leaves are no longer limited by potential electron transport. Instead, RuBP carboxylation activity becomes limiting, which in turn is related to leaf N content. Figure 6 shows diurnal rates of assimilation (μmol CO_2 s^{-1} per layer) and internal CO_2 concentrations (C_i, μmol mol^{-1}) in selected layers on day 215.

After midday a third factor becomes limiting. In the first few hours of daylight the transpirational demand created by stomatal opening is met from water stored in the leaves and the crown (i.e. capacitance). However, once the stored water is exhausted, the leaves must be supplied by water transported from the roots. In the upper canopy, over 20 m above the forest floor, xylem hydraulic resistance is significant and stomata are forced to close to maintain turgor and avoid xylem cavitation. Because afternoon atmospheric saturation deficits are high in the upper canopy, the degree of stomatal closure required to maintain turgor has a significant effect on CO_2 diffusion into upper canopy layers.

Further factors involved in reducing afternoon *NEE* include the measured drop in ambient CO_2 concentration resulting from CO_2 uptake by the canopy, and the recorded increase in soil respiration caused by higher afternoon soil temperatures. However, the model suggests that the overriding reduction in afternoon CO_2 uptake results from stomatal closure in the upper canopy caused by restrictions in water supply. Measured and modelled *NEE* show a similar hyperbolic response to incident PPFD during the four days we examined (Fig. 7), and both show the same hysteresis, with afternoon CO_2 uptake lower than morning uptake at a similar PPFD.

Deeper in the canopy, there are different limitations to productivity. Light levels are lower, but so also are atmospheric saturation deficits, temperatures and wind speeds, and hydraulic resistance is reduced in layers nearer the ground. Therefore water demand in the lower canopy never exceeds supply, and there is no stomatal closure during the afternoon according to the model.

In their studies on gas exchange in mature *Quercus rubra*, Weber & Gates (1990) showed that a marked midday depression in CO_2 assimilation commonly occurred

Table 1. Parameter values and variables used in the soil-plant-atmosphere model

Parameter/variable	Symbol	Units	Value	Source
Net assimilation rate	A	μmol m^{-2} s^{-1}	variable	Eqn A10
Ambient atmospheric CO_2 concentration	C_a	μmol mol^{-1}	variable	measurement data
Mesophyll CO_2 concentration	C_c	μmol mol^{-1}	variable	equilibrate diffusion and metabolic uptake of CO_2
Leaf internal CO_2 concentration	C_i	μmol mol^{-1}	variable	Calculate from A, C_c and g_s
Canopy layer capacitance	C_n	mmol MPa^{-1} m^{-2}	8000	Schulze *et al.* (1985)
Transpiration from canopy layer n	E_n	mmol m^{-2} s^{-1}	variable	Penman–Monteith equation
Accleration due to gravity	g	m s^{-2}	9·8	
Leaf boundary layer conductance to water vapour	g_b	m s^{-1}	variable	Eqn from Nobel (1983)
Mesophyll conductance	g_i	m s^{-1}	0·0025	Epron *et al.* (1995)
Stomatal conductance	g_s	m s^{-1}	variable	see text
Total conductance to CO_2 from atmosphere to mesophyll	g_t	mol m^{-2} s^{-1}	variable	Eqn A11
Canopy hydraulic conductivity	G_p	mmol m^{-1} s^{-1} MPa^{-1}	4·5	Tyree & Sperry (1988)
Layer height	h	m	10–24	site estimate
Relative humidity	H	%	variable	measurement data
Maximum electron transport rate	J_{max}	μmol m^{-2} s^{-1}	variable	Eqn 3
Canopy layer water flux	J_n	μmol m^{-2} s^{-1}	variable	Eqn A5
RuBP carboxylation capacity temperature coefficient	k_{tc}		1·0 at 30°C	McMurtrie *et al.* (1992)
Electron transport temperature coefficient	k_{tj}		1·0 at 30°C	McMurtrie *et al.* (1992)
Michaelis–Menten constant of Rubisco for CO_2 at 25°C	K_c	μmol mol^{-1}	310	Kirschbaum & Farquhar (1984)
Inhibition constant of Rubisco by O_2 at 25°C	K_o	mmol mol^{-1}	155	Kirschbaum & Farquhar (1984)
Leaf area index	L	m^2 m^{-2}	3·5	1992 site leaf litter
Fine root length per m^2 ground area; total/layer	l_R/l_r	m m^{-2}	1300/130	McClaugherty *et al.* (1982)
Soil hydraulic conductivity	L_{soil}	mmol m^{-1} s^{-1} MPa^{-1}	2·4	Boone (personal communication), Saxton *et al.* (1986)
Areal concentration of leaf N	N	g m^{-2} *ground area*	6·76	Aber *et al.* (1993), Amthor *et al.* (1994)
Foliar N concentration in layer n	N_n	g m^{-2} *leaf area*	variable	Eqn A1
Proportion of total canopy N in top layer	n_{top}		0·152	Ellsworth & Reich (1993)
Slope coefficient of canopy N distribution	n_{sl}		–0·103	Ellsworth & Reich (1993)
Atmospheric pressure	P	Pa	~1x10^5	
Respiration rate	R_d	μmol m^{-2} s^{-1}	variable	Ryan (1991)
Canopy layer hydraulic resistance	R_{pn}	MPa s m^2 mmol^{-1}	variable	Eqn A3
Soil hydraulic resistance to canopy layer n	R_{sn}	MPa s m^2 mmol^{-1}	0·0025	Eqn A2
Gas constant	R	Pa m^3 mol^{-1} K^{-1}	8·3144	Jones (1992)
Fine root radius	r_r	m	0·00035	McClaugherty *et al.* (1982)
Radius of soil cylinder exploited by a root	r_s	m	$(1/\pi l_r)^{1/2}$	
Air temperature	T_a	°C	variable	measurement data
Leaf temperature	T_l	°C	variable	steady-state approximation (Jones 1992)
Soil temperature	T_s	°C	variable	measurement data
Actual rate of carboxylation	V_c	μmol m^{-2} s^{-1}	variable	Farquhar & Von Caemmerer (1982)
RuBP carboxylation capacity	V_{cmax}	μmol m^{-2} s^{-1}	variable	Eqn 2
Canopy layer water content	W_n	mmol m^{-2}	8800	Schulze *et al.* (1985)
Atmospheric saturation deficit in canopy layer	δe	kPa	variable	measurement data
CO_2 compensation point with $R_d = 0$ at 25°C	Γ^*	μmol mol^{-1}	36·5	Epron *et al.* (1995)
$\delta A/\delta g_s$ threshold for stomatal opening	ι	%	0·07	conjecture
RuBP carboxylation catalytic rate coefficient at 30°C	κ_c	μmol g^{-1} s^{-1}	33·6	see text
Electron transport rate coefficient at 30°C	κ_j	μmol g^{-1} s^{-1}	44·3	see text
Density of water	ρ_w	kg m^{-3}	998·2	Jones (1992)
Minimum sustainable leaf water potential	Ψ_{lmin}	MPa	–2·5	Bassow (1995)
Leaf water potential in layer n	Ψ_{ln}	MPa	variable	Eqns 1 & A9
Soil water potential	Ψ_s	MPa	–0·01	Boone (personal communication), Saxton *et al.* (1986)

during summers in the upper canopy. Reich *et al.* (1990) report similar patterns in their investigation of oak–maple forests. Leaf-level measurements of photosynthesis in the upper and lower canopy have been undertaken at Harvard Forest in 1991 and 1992 (Bassow 1995). The data show a high degree of variability. However, the measurements do indicate that CO_2 assimilation in the upper canopy tended to decline after midday. In the sub-canopy, assimilation

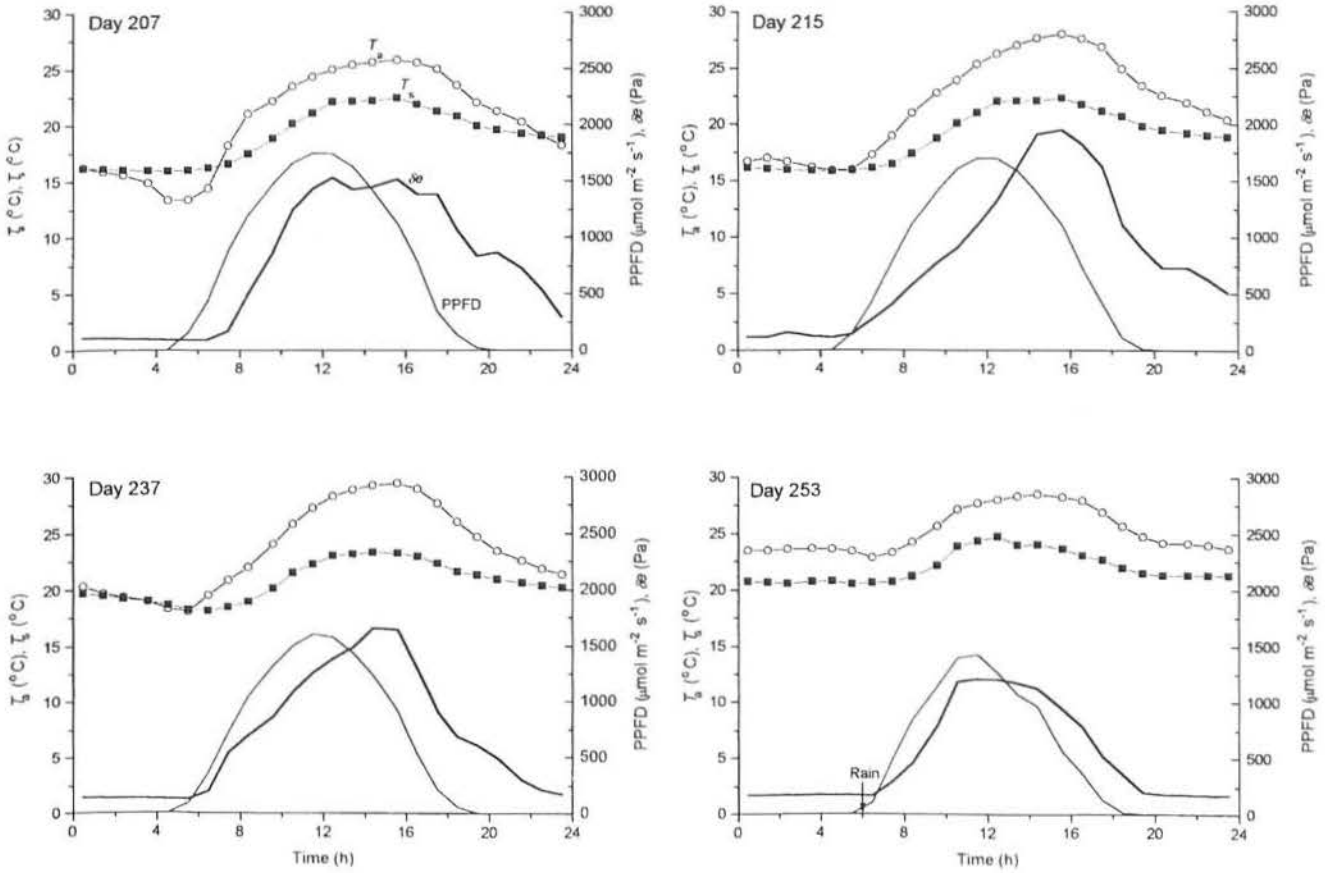

Figure 5. Diurnal course of measured environmental variables during four days in 1992. The graphs show δe, atmospheric saturation deficit (——), T_a, air temperature (–○–), T_s, soil temperature (–■–) and PPFD, photosynthetic photon flux density (——).

rates were generally lower, but less variable throughout the day, and an afternoon decline in uptake was not indicated. These data provide qualitative substantiation for the model results at the canopy layer level.

Bearing in mind the magnitude of the error associated with eddy correlation methods, it is also instructive to examine where modelled and measured results for the whole canopy diverge. For day 253 (Fig. 4) the model underestimates CO_2 uptake and *LE* during the middle of the day. However, this day was characterized by a great degree of variability in flux measurements, and by relatively high soil temperatures. It seems likely that our estimates of soil respiration are an overestimate. The morning peak in measured *LE* is explained by evaporation from wet leaf surfaces resulting from rainfall at 0600 h.

Internal CO_2 concentration (C_i)

Figure 6 traces the diurnal course of predicted internal CO_2 concentrations (C_i) for five canopy layers on day 215. Tenhunen *et al.* (1984) observe that C_i tends to remain essentially constant despite stomatal closure, so that assimilation and conductance change in concert. This observation is the basis of some empirical models of g_s (Ball *et al.* 1987).

A similar coordination between assimilation and stomatal conductance arises because of the optimization we use to calculate g_s in our model. Thus, in our model C_i remains relatively constant for much of the day and in most layers, between 260 and 280 μmol mol^{-1}, a typical range for C_3 leaves. However, in topmost layers, where afternoon g_s is set to avoid cavitation rather than optimise C uptake, C_i falls as diffusion becomes limiting to assimilation. In studies of gas exchange in mature *Quercus rubra*, Weber & Gates (1990) showed that C_i did decline during the middle of the day, though not to the extent of our predictions for the upper canopy.

The stable C_i values predicted for each layer are similar, their exact values dependent on foliar N concentration and incident radiation. However, because the impacts of stomatal closure due to water stress are confined to the upper canopy, the average daily C_i will decline with height. Carbon isotope ratios in leaves can provide an indication of long-term aggregated C_i values (Farquhar *et al.* 1989). Using this technique, Yoder *et al.* (1994) have shown that in upper canopy trees there is evidence of reduced C_i, which they trace to hydraulic limitations. Although their data pertain to a coniferous stand at a dry site, they do provide some support for our simulated vertical distribution of average C_i in developed stands.

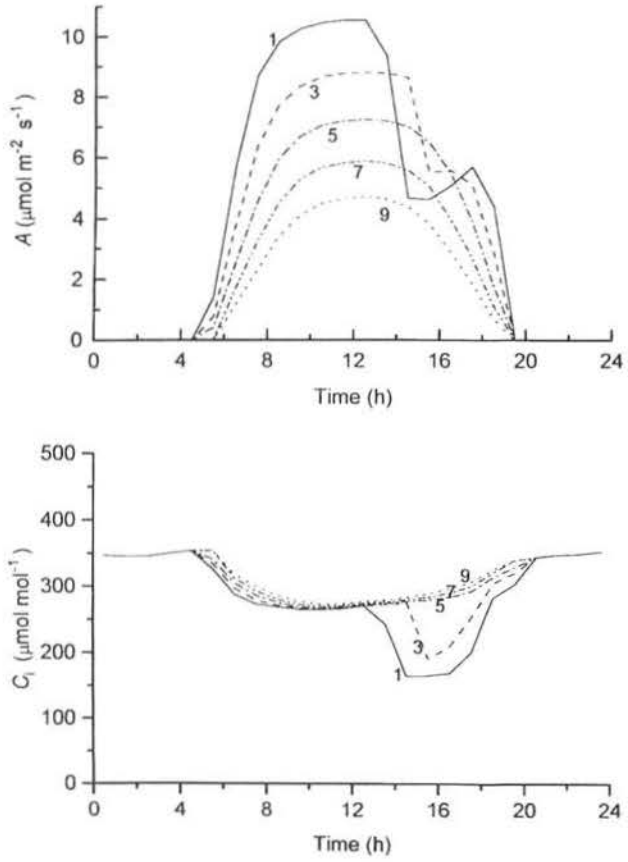

Figure 6. Variation in total carbon assimilation rate (top) and internal CO_2 concentration (bottom) of five out of the 10 simulated canopy layers through the course of day 215. The layers are marked from the top layer (1) to the second from the bottom (9).

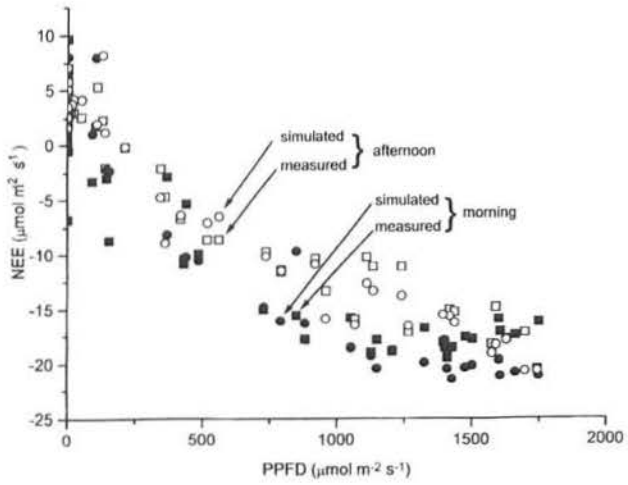

Figure 7. Daytime simulated (circles) and measured (squares) net ecosystem exchange of CO_2 as a function of mean hourly incident PPFD during each hour for four days during the summer of 1992 when winds were from the south-west. Morning rates are indicated by closed symbols and afternoon rates by open symbols.

Stomatal conductance

Canopy models have employed empirically derived relationships (Ball *et al.* 1987; Collatz *et al.* 1991) to predict stomatal conductance (mol m^{-2} s^{-1}), using variations on the equation

$$g_s = mAH_s/C_s + b, \quad (4)$$

where H_s is relative humidity at the leaf surface (%), C_s is CO_2 concentration at the leaf surface (μmol mol^{-1}), A is net assimilation rate (μmol m^{-2} s^{-1}), and m (dimensionless) and b (mol m^{-2} s^{-1}) are constants. We plot our predictions of g_s for each layer of the canopy through the course of one day (215) against AH/C_a (see Fig. 8) – because of high leaf boundary layer conductances, ambient and surface values of humidity and CO_2 concentration will not differ greatly. The figure shows that our model of g_s is clearly related ($r^2 = 0{\cdot}83$) to the empirical function. The gradient of a fitted line, given that b is small, gives an estimate of m of 0·12, which is in accordance with published values (McMurtrie 1993). However, our model does display an obvious excursion from the Ball *et al.* relation; this is because Eqn 4 is not dependent in any way on plant water status.

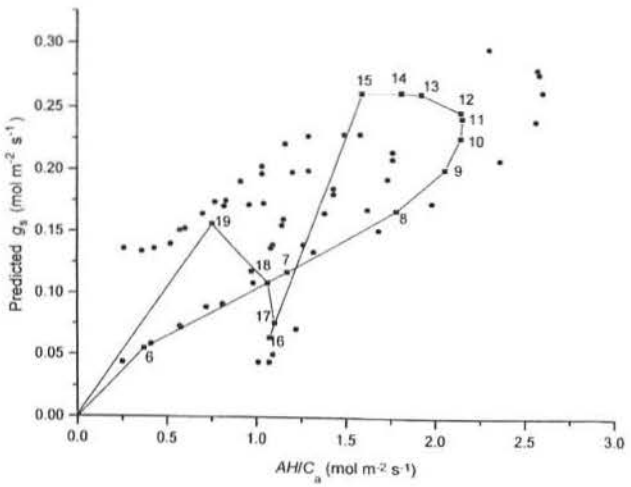

Figure 8. Predicted stomatal conductance for five layers on day 215 (•), as a function of the Ball–Berry relationship (Ball *et al.* 1987), where A is canopy layer CO_2 assimilation rate, H is ambient humidity and C_a is ambient air CO_2 concentration. Also shown is the diurnal course of stomatal conductance for the third layer into the canopy (–■–); the numbers indicate the time of day (h).

The model can also be used to examine how g_s varies within the plant canopy. Daylight average and maximum g_s are plotted against leaf height for the same day (Fig. 9). Maximum g_s declines deeper into the canopy. However, the greater water stress in the upper canopy and the resulting afternoon stomatal closure mean that average g_s is highest below the topmost layer. These predictions are in agreement with the measurements of Roberts *et al.* (1990)

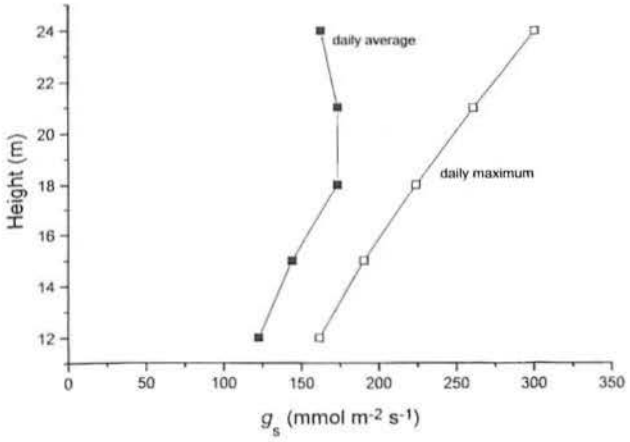

Figure 9. The variation of daily maximum (○) and average (■) predicted stomatal conductance with depth in the canopy on day 215.

who examined variation in g_s with height in a tropical rain forest. Plants higher in the canopy exhibited the greatest maximum g_s values, and showed a steep decline after a mid-morning peak. Plants nearer the forest floor had lower maximum g_s values and showed far less diurnal variation. These data do indicate that the predicted patterns are consistent with observations from other tall-stature forests.

Nitrogen use efficiency

Nitrogen use efficiency (*NUE*) of each canopy layer through a single day is determined as the total gross CO_2 assimilation per g foliar N. Integrated daily *NUE*s of the canopy layers are similar (see Fig. 10), suggesting that the N distribution we applied is close to optimal. Upper layers are the most efficient early and late in the day, when they are better illuminated and least water-stressed. Lower layers are the most efficient around noon, when irradiance is highest. The *NUE* of the topmost layers declines precipitously with the onset of stomatal closure induced by water stress. The model indicates that taking account of hydraulic limitations to productivity in the upper layers may be important in determining the optimal distribution of N within the canopy.

Sensitivity analysis

The parameters tested for sensitivity are those related to the hydraulic model and stomatal variation that were not measured at the site; C_n, Ψ_{lmin}, G_p and ι. The model was rerun for the 25 d, with these parameters varied individually by at least ±30% (according to uncertainty about the parameter estimates). Table 2 shows the r^2 and slopes ± standard errors of the measured versus predicted fluxes when winds were from the south-west. There was only a small alteration in model response with variation in canopy hydraulic conductivity (G_p), and canopy layer capacitance (C_n). There was more sensitivity to changes in minimum sustainable leaf water potential (Ψ_{lmin}). When this was increased to −1·5 MPa, transpiration and photosynthesis were significantly reduced, because stomatal opening is constrained as Ψ_{lmin} becomes less negative. Less negative values of Ψ_{lmin} are equivalent to more nega-

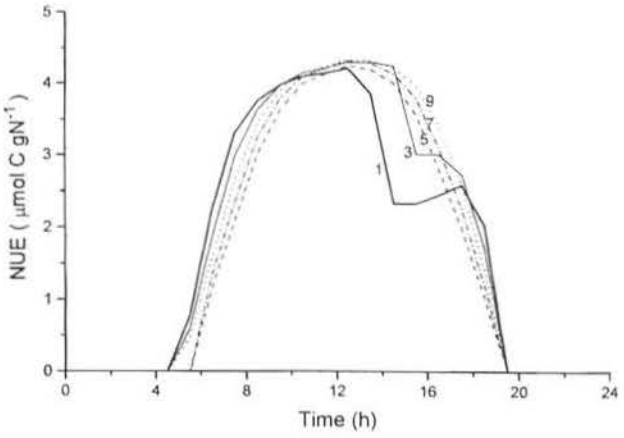

Figure 10. Diurnal variation in nitrogen use efficiency (μmol C assimilated.d^{-1} g^{-1} foliar N) for five of the 10 layers on day 215. The layers are numbered from the topmost (1) to the second from bottom (9).

Parameter		Value	LE		NEE	
			r^2	slope	r^2	slope
Standard			0·87	1·01±0·02	0·86	1·03±0·02
G_p	(4·5)	3·0	0·87	0·97±0·02	0·86	1·00±0·02
		6·0	0·87	1·04±0·02	0·86	1·04±0·02
Ψ_{lmin}	(−2·5)	−3·5	0·85	1·08±0·02	0·85	1·06±0·02
		−1·5	0·80	0·80±0·02	0·83	0·92±0·02
C	(8000)	11000	0·86	1·06±0·02	0·86	1·05±0·02
		5000	0·86	0·93±0·02	0·86	1·00±0·02
ι	(0·07)	0·01	0·82	1·25±0·03	0·86	1·06±0·02
		0·20	0·87	0·82±0·02	0·86	0·96±0·02

Table 2. Sensitivity analysis of the canopy model for canopy hydraulic conductance coefficient (G_p), minimum leaf water potential (Ψ_{lmin}), canopy layer capacitance (C_n) and stomatal threshold (ι); bracketed values are those from the standard parameter set. The model was rerun for the subset of 25 days in 1992 when winds were from the southwest, with altered parameter values as indicated. We determined r^2 and slope ± standard error from linear regression of measured (independent) versus modelled (dependent) fluxes (latent energy and net ecosystem exchange), fitted through the origin (n = 140)

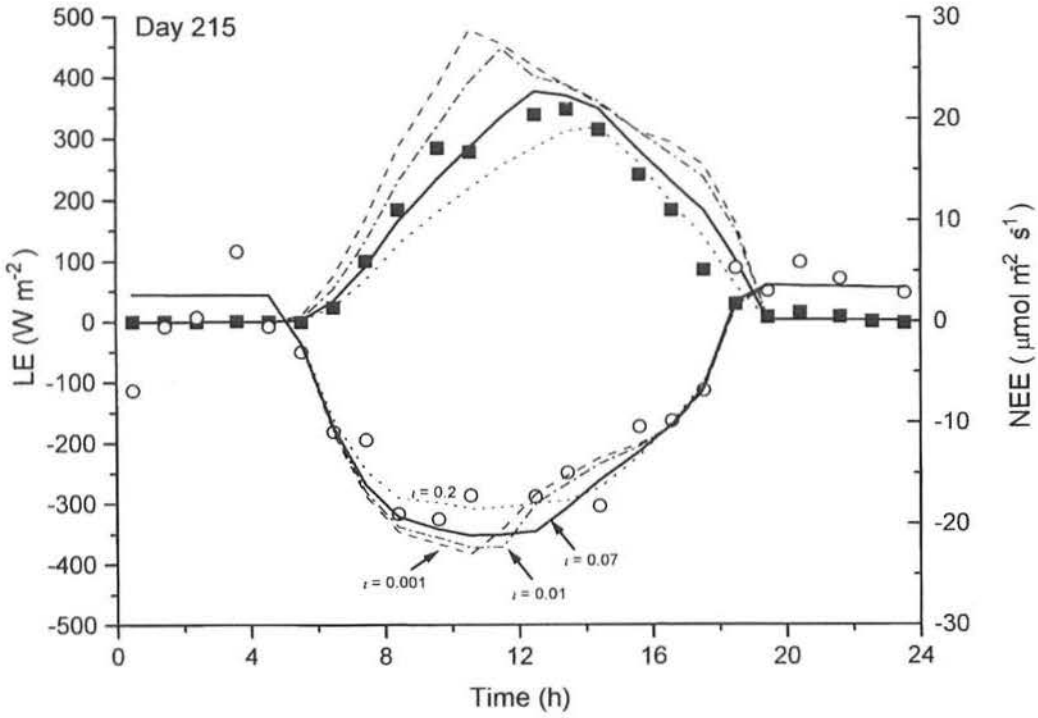

Figure 11. The sensitivity of the simulated net ecosystem exchange and latent energy to variation in t, the stomatal threshold parameter, on day 215. Measured values of *NEE* (○) and *LE* (■) are indicated. The lines show the predicted diurnal course of *LE* (top) and *NEE* (bottom) with t set to 0·2 (------) 0·07 (——) 0·01 (– · – · –) and 0·001 (– – – –).

tive values of Ψ_s. Thus, sensitivity analysis of Ψ_{lmin} also serves as a sensitivity analysis on soil water availability.

LE showed more sensitivity than *NEE* to variation in t, the stomatal threshold parameter that controls water use efficiency. We have used t to constrain g_s, arguing that conservation of the plant water store ameliorates afternoon water stress. The sensitivity of this parameter (set to 0·07% in the model runs) and this assumption were tested in more detail. For day 215 the canopy model was rerun with a variety of t values, ranging from 0·001 to 0·2% (Fig. 11). With lower t values, GPP (gross primary productivity) was stimulated in the morning because stomata opened wider. The model then forecast a rapid exhaustion of the water store, causing stomatal closure to occur earlier and to affect more of the canopy. Afternoon GPP was significantly reduced, and so in balance there was minimal improvement (less than 1%) in daily total GPP with less constrained g_s. With higher values of t, the model predicted that stomata opened less widely in the morning; water stress was ameliorated in the afternoon, but this highly conservative strategy reduced daily GPP overall. The hydraulic model does set short-term limits on productivity, but suggests that conservative g_s limits the degree of canopy water stress.

Further directions

The model does not include any representation of water dynamics around roots or the impacts of root clumping (Tardieu *et al.* 1992). Water uptake rates may be affected by the development and enlargement of water-depletion zones around roots during the course of the day. If morning photosynthesis relies largely on stored water, these depletion zones around roots are expected to affect only afternoon transpiration and therefore might explain the tendency of the model to overestimate late afternoon *LE*. Also, we did not simulate the variation in soil moisture at different depths. To test and apply this model further, we require data from a water-stressed site, so that the impacts of low soil moisture on canopy processes can be examined.

The major objective of this work was to develop predictions of canopy fluxes, both for use in investigation of the stand-level response to global change, and for application to ecosystem models (e.g. Parton *et al.* 1988; Rastetter *et al.* 1991). Having confirmed model predictions against whole-forest measurements, we can reliably use the model to develop more aggregated representations of canopy processes. These are much simpler sets of equations, operating like a simplified 'big-leaf' model, that capture the behaviour of the process-based formulation while requiring many fewer parameters and much reduced computing power.

CONCLUSIONS

We describe a soil–plant–atmosphere continuum model that, given numerous simplifications and assumptions, adequately predicts both canopy CO_2 uptake and transpira-

tion for a *Quercus–Acer* site at Harvard Forest. The model successfully captures the impacts of contrasting weather conditions on C assimilation and *LE* flux over a growing season. Thus, we can confidently employ the model to simulate seasonal patterns of C and water exchanges, given the availability of relevant parameters.

The model successfully accounts for the observed afternoon decline in CO_2 uptake, suggesting that this arises from stomatal closure in the upper canopy, initiated by exhaustion of stored water. Because the impacts of water stress are confined to the upper canopy, where atmospheric demand is highest, and hydraulic resistance greatest, the model suggests that average daily internal CO_2 concentrations (C_i) decline with height. The predictions of this model for g_s are broadly in agreement with those of the Ball *et al.* (1987) approach, though differences do arise because of the impacts of plant water status on g_s in our model. Our simulated maximum g_s values decline with foliar N concentration and with canopy height. Examination of predicted N use efficiencies shows that the measured N distribution applied in this model is close to optimal. Further, sensitivity analysis of the hydraulic parameters shows that gas fluxes are most responsive to variation in minimum leaf water potential ($\Psi_{l\min}$) and soil water potential (Ψ_s). Analysis also reveals that an optimal stomatal behaviour may exist, which most efficiently utilizes stored water to delay the onset of afternoon water stress.

ACKNOWLEDGMENTS

We are very grateful to Susan Bassow for access to results of her Ph.D. research. Thanks are also due to Bob McKane, Chuck Hopkinson, Rich Boone, Joe Vallino, Bill Currie, Barbara Yoder, Mike Ryan, Joe Landsberg and two anonymous reviewers for their input. This research was conducted at the MBL with funding from US National Science Foundation (DEB-9307888) and US Environmental Protection Agency (CR81863301–1). Measurements at Harvard Forest were supported by US National Science Foundation (BSR-8919300, DEB-9411975), the US National Aeronautic and Space Administration (NAGW-3082), the US Department of Energy through the North East Regional Center of the National Institute for Global Environmental Change (DOE co-operative agreement EE-FCO3–90ER61010) and by Harvard University (Harvard Forest and Division of Applied Sciences).

REFERENCES

Aber J.D. (1979) Foliage-height profiles and succession in northern hardwood forests. *Ecology* **60,** 18–23.

Aber J.D., Magill A., Boone R., Melillo J.M., Steudler P. & Bowden R. (1993) Plant and soil responses to chronic nitrogen addition at the Harvard Forest, Massachusetts. *Ecological Applications* **3,** 156–166.

Amthor J.S. (1994) Scaling CO_2-photosynthesis relationships from the leaf to the canopy. *Photosynthesis Research* **39,** 321–350.

Amthor J.S., Goulden M.L., Munger J.W. & Wofsy S.C. (1994) Testing a mechanistic model of forest-canopy mass and energy exchange using eddy correlation: carbon dioxide and ozone uptake by a mixed oak-maple stand. *Australian Journal of Plant Physiology* **21,** 623–651.

Aston M.J. & Lawlor D.W. (1979) The relationship between transpiration, root water uptake and leaf water potential. *Journal of Experimental Botany* **30,** 169–181.

Baldocchi D. (1992) A lagrangian random-walk model for simulating water vapor, CO_2 and sensible heat flux densities and scalar profiles over and within a soybean canopy. *Boundary-Layer Meteorology* **61,** 113–144.

Baldocchi D.D., Hutchison B.A., Matt D.R. & McMillen R.T. (1985) Canopy radiative transfer models for spherical and known leaf inclination angle distributions: a test in an oak-hickory forest. *Journal of Applied Ecology* **22,** 539–555.

Baldocchi D.D., Hicks B.B. & Meyers T.P. (1988) Measuring biosphere-atmosphere exchanges of biologically related gases with micrometeorological methods. *Ecology* **69,** 1331–1340.

Ball J.T., Woodrow I.E. & Berry J.A. (1987) A model predicting stomatal conductance and its contribution to the control of photosynthesis under different environmental conditions. In *Progress in Photosynthesis Research*, Vol. IV (ed. J. Biggins), pp. 221–224. Martinus Nijhoff, Dordrecht.

Bassow S.L. (1995) *Canopy photosynthesis and carbon cycling in a deciduous forest: implications of species composition and rising concentrations of CO_2*. PhD thesis, Department of Organismic and Evolutionary Biology, Harvard University.

Cionco R.M. (1985) Modeling windfields and surface layer wind profiles over complex terrain and within vegetative canopies. In *The Forest–Atmosphere Interaction* (eds B. A. Hutchison and B. B. Hicks), pp. 501–52. Reidel, Dordrecht.

Cochard H. & Tyree M.T. (1990) Xylem dysfunction in *Quercus*: vessel sizes, tyloses, cavitation and seasonal changes in embolism. *Tree Physiology* **6,** 393–407.

Collatz C.G., Ball J.T., Grivet C. & Berry J.A. (1991) Physiological and environmental regulation of stomatal conductance, photosynthesis and transpiration: a model that includes a laminar boundary layer. *Agricultural and Forest Meteorology* **54,** 107–136.

Cornic G., Le Gouallec, J.-L., Briantais J.M. & Hodges M. (1989) Effect of dehydration and high light on photosynthesis of two C_3 plants (*Phaseolus vulgaris* L. & *Elatostema repens* (Lour.) Hall f.). *Planta* **177,** 84–90.

Cowan I.R. (1965) Transport of water in the soil–plant–atmosphere system. *Journal of Applied Ecology* **2,** 221–239.

Cowan I.R. (1977) Stomatal behaviour and environment. *Advances in Botanical Research* **4,** 117–228.

Ellsworth D.S. & Reich P.B. (1993) Canopy structure and vertical patterns of photosynthesis and related leaf traits in a deciduous forest. *Oecologia* **96,** 169–178.

Epron D., Godard D., Cornic C. & Genty B. (1995) Limitation of net CO_2 assimilation rate by internal resistances to CO_2 transfer in the leaves of two tree species (*Fagus sylvatica* L. & *Castanea sativa* Mill.). *Plant, Cell and Environment* **18,** 43–52.

Epron D. & Dreyer E. (1993) Photosynthesis of oak leaves under water stress: maintenance of high photochemical efficiency of photosystem II and occurrence of non-uniform CO_2 assimilation. *Tree Physiology* **13,** 107–117.

Erbs D.G., Klein S.A. & Duffie J.A. (1982) Estimation of the diffuse radiation fraction for hourly, daily and monthly average global radiation. *Solar Energy* **28,** 293–302.

Farquhar G.D. (1989) Models of integrated photosynthesis of cells and leaves. *Philosophical Transactions of the Royal Society of London B* **323,** 357–367.

Farquhar G.D., Ehleringer J.R. & Hubick K.T. (1989) Carbon isotope discrimination and photosynthesis. *Annual Reviews of Plant Physiology and Molecular Biology* **40,** 503–537.

Farquhar G.D. & Von Caemmerer S. (1982) Modelling of photosynthetic response to the environment. In *Physiological Plant Ecology II. Encyclopedia of Plant Physiology, New Series*, Vol. 12B (eds O. L. Lange, P. S. Nobel, C. B. Osmond & H. Ziegler), pp. 549–587. Springer-Verlag, Berlin.

Farquhar G.D. & Wong S.C. (1984) An empirical model of stomatal conductance. *Australian Journal of Plant Physiology* **11,** 191–210.

Federer C.A. (1979) A soil–plant–atmosphere model for transpiration and availability of soil water. *Water Resources Research* **15,** 555–562.

Field C.B. (1991) Ecological scaling of carbon gain to stress and resource availability. In *Response of Plants to Multiple Stress* (eds H. A. Mooney, W. E. Winner & E. J. Pell), pp. 35–65. Academic Press, San Diego.

Field C.B. & Mooney H.A. (1986) The photosynthesis-nitrogen relationship in wild plants. In *On the Economy of Plant Form and Function* (ed. T. J. Givnish), pp. 25–55. Cambridge University Press, Cambridge.

Gollan T., Turner N.C. & Schulze, E.-D. (1985) The response of stomata and leaf gas exchange to vapour pressure deficits and soil water content III. In the sclerophyllous woody species *Nerium oleander*. *Oecologia* **65,** 356–362.

Goulden ML, Munger JW, Fan S-M, Daube BC, and Wofsy SC. (1996) Measurements of carbon storage by long-term eddy correlation: Methods and a critical evaluation of accuracy. *Global Change Biology*, in press.

Harley P.C., Thomas R.B., Reynolds J.F. & Strain B.R. (1992) Modelling photosynthesis of cotton grown in elevated CO_2. *Plant, Cell and Environment* **15,** 271–282.

Hellkvist J., Richards G.P. & Jarvis P.G. (1974) Vertical gradients of water potential and tissue water relations in sitka spruce trees measured with the pressure chamber. *Journal of Applied Ecology* **11,** 637–667.

Jarvis P.G., Miranda H.S. & Muetzenfeldt R.I. (1985) Modelling canopy exchanges of water vapour and carbon dioxide in coniferous forest plantations. In *The Forest–Atmosphere Interaction* (eds B. A. Hutchison & B. B. Hicks), pp. 521–54. Reidel, Dordrecht.

Jones H.G. (1978) Modelling diurnal trends of leaf water potential in transpiring wheat. *Journal of Applied Ecology* **15,** 613–626.

Jones H.G. (1992) *Plants and Microclimate*. Cambridge University Press, Cambridge.

Jones H.G. & Sutherland R.A. (1991) Stomatal control of xylem embolism. *Plant, Cell and Environment* **14,** 607–612.

Kirschbaum M.U.F. & Farquhar G.D. (1984) Temperature dependence of whole leaf photosynthesis in *Eucalyptus pauciflora* Sieb. ex Spreng. *Australian Journal of Plant Physiology* **11,** 519–538.

Kuppers M. (1984) Carbon relations and competition between woody species in a Central European hedgerow. *Oecologia* **64,** 344–354.

Landsberg J.J., Blanchard T.W. & Warrit B. (1976) Studies on the movement of water through apple trees. *Journal of Experimental Botany* **27,** 579–596.

Loreto F. & Sharkey T.D. (1990) A gas-exchange study of photosynthesis and isoprene emission in *Quercus rubra* L. *Planta* **182,** 523–531.

McClaugherty C.A., Aber J.D. & Melillo J.M. (1982) The role of fine roots in the organic matter and nitrogen budgets of two forest ecosystems. *Ecology* **63,** 1481–1490.

McMurtrie R.E., Comins H.N., Kirschbaum M.U.F. & Wang, Y.-P. (1992) Modifying existing forest growth models to take account of effects of elevated CO_2. *Australian Journal of Botany* **40,** 657–677.

McMurtrie R.E. (1993) Modelling of canopy carbon and water balance. In *Photosynthesis and Production in a Changing Environment: a Field and Laboratory Manual* (eds D. O. Hall, J. M. O. Scurlock, H. R. Bolhar-Nordenkampf, R. C. Leegood & S. P. Long), pp. 220–231. Chapman & Hall, London.

Meinzer F.C. & Grantz D.A. (1990) Stomatal and hydraulic conductance in growing sugarcane: stomatal adjustment to water transport capacity. *Plant, Cell and Environment* **13,** 383–388.

Meinzer F.C. & Grantz D.A. *(1991)* Coordination of stomatal, hydraulic, and canopy boundary layer properties: Do stomata balance conductances by measuring transpiration? *Physiologia Plantarum* **83,** 324–329.

Newman E.I. (1969) Resistance to water flow in soil and plant. I. Soil resistance in relation to amounts of root: theoretical estimates. *Journal of Applied Ecology* **6,** 1–12.

Nobel P.S. (1983) *Biophysical Plant Physiology and Ecology*. W.H.Freeman, New York.

Norman J.M. & Polley W. (1989) Canopy photosynthesis. In *Photosynthesis* (ed. W. R. Briggs), pp. 227–241. Alan R. Liss, New York.

O'Neill R.V. & Rust B. (1979) Aggregation error in ecological models. *Ecological Modelling* **7,** 91–105.

Oren R., Schulze, E.-D., Matyssek R. & Zimmermann R. (1986) Estimating photosynthetic rate and annual carbon gain in conifers from specific leaf weight and leaf biomass. *Oecologia* **70,** 187–193.

Parton W.J., Stewart J.W.B. & Cole C.V. (1988) Dynamics of C, N, P and S in grassland soils: A model. *Biogeochemistry* **5,** 109–131.

Passioura J.B. (1982) Water in the soil–plant–atmosphere continuum. In *Physiological Plant Ecology II. Encyclopedia of Plant Physiology, New Series*, Vol. 12B (eds O. L. Lange, P. S. Nobel, C. B. Osmond & H. Ziegler), pp. 5–33. Springer-Verlag, Berlin.

Rastetter E.B., Ryan M.G., Shaver G.R., Melillo J.M., Nadelhoffer K.J., Hobbie J.E. & Aber J.D. (1991) A general biogeochemical model describing the responses of the C and N cycles in terrestrial ecosystems to changes in CO_2, climate, and N deposition. *Tree Physiology* **9,** 101–126.

Rastetter E.B., King A.W., Cosby B.J., Hornberger G.M., O'Neill R.V. & Hobbie J.E. (1992) Aggregating fine-scale ecological knowledge to model coarser-scale attributes of ecosystems. *Ecological Applications* **2,** 55–70.

Raupach M.R. & Finnigan J.J. (1988) 'Single-layer models of evaporation from plant canopies are incorrect but useful, whereas mulitlayer models are correct but useless': Discuss. *Australian Journal of Plant Physiology* **15,** 705–716.

Reich P.B., Ellsworth D.S., Kloeppel B.D., Fownes J.H. & Gower S.T. (1990) Vertical variationin canopy structure and CO_2 exchange of oak-maple forests: influence of ozone, nitrogen, and other factors on simulated carbon gain. *Tree Physiology* **7,** 329–345.

Ren Z. & Sucoff E. (1995) Water movement through *Quercus rubra* l. Leaf water potential and conductance during polycyclic growth. *Plant, Cell and Environment* **18,** 447–462.

Roberts J., Cabral O.M.R. & de Aguiar L.F. (1990) Stomatal and boundary-layer conductances in an Amazonian terra firme rain forest. *Journal of Applied Ecology* **27,** 336–353.

Running S.W. & Coughlan J.C. (1988) A general model of forest ecosystem processes for regional applications. I. Hydrologic balance, canopy gas exchange and primary production processes. *Ecological Modelling* **42,** 125–154.

Russell G., Jarvis P.G. & Montieth J.L. (1989) Absorption of radiation by canopies and stand growth. In *Plant Canopies: Their Growth, Form and Function* (eds G. Russell, B. Marshall & P. G. Jarvis), pp. 21–40. Cambridge University Press, Cambridge.

Ryan M.G. (1991) The effect of climate change on plant respiration. *Ecological Applications* **1,** 157–167.

Saxton K.E., Rawls W.J., Romberger J.S. & Papendick R.I. (1986) Estimating generalized soil-water characteristics from texture. *Soil Science Society of America Journal* **90,** 1031–1036.

Schimel D.S. (1995) Terrestrial ecosystems and the carbon cycle. *Global Change Biology* **1,** 77–91.

Schulze, E.-D., Cermak J., Matyssek R., Penka M., Zimmermann R., Vasicke F., Gries W. & Kucera J. (1985) Canopy transpiration and water fluxes in the xylem of the trunk of *Larix* and *Picea* trees – a comparison of xylem flow, porometer and cuvette measurements. *Oecologia* **66,** 475–483.

Shinozaki K., Yoda K. & Hozumi K. (1964) A quantitative analysis of plant form: the pipe model theory. *Japanese Journal of Ecology* **14,** 97–105.

Sinclair T.R., Murphy C.E.J. & Knoerr K.R. (1976) Development and evaluation of simplified models for simulating canopy photosynthesis and transpiration. *Journal of Applied Ecology* **13,** 813–829.

Szeicz G. (1974) Solar radiation in plant canopies. *Journal of Applied Ecology* **11,** 1117–1156.

Tardieu F., Bruckler L. & Lafolie F. (1992) Root clumping may affect the root water potential and the resistance to soil-root water transport. *Plant and Soil* **140,** 291–301.

Tenhunen J.D., Lange O.L., Gebel J., Beyschlag W. & Weber J.A. (1984) Changes in photosynthetic capacity, carboxylation efficiency, and CO_2 compensation point associated with midday stomatal closure and midday depression of net CO_2 exchange of leaves of *Quercus suber*. *Planta* **162,** 193–203.

Tyree M.T. (1988) A dynamic model for water flow in a single tree: evidence that models must account for hydraulic architecture. *Tree Physiology* **4,** 195–217.

Tyree M.T. & Dixon M.A. (1986) Water stress induced cavitation and embolism in some woody plants. *Physiologia Plantarum* **66,** 397–405.

Tyree M.T. & Sperry J.S. *(1988)* Do woody plants operate near the point of catastrophic xylem dysfunction caused by dynamic water stress? *Plant Physiology* **88,** 574–580.

Tyree M.T. & Sperry J.S. (1989) Vulnerability of xylem to cavitation and embolism. *Annual Reviews of Plant Physiology and Molecular Biology* **40,** 19–38.

Von Caemmerer S. & Farquhar G.D. (1981) Some relationships between the biochemistry of photosynthesis and the gas exchange of leaves. *Planta* **153,** 376–387.

Weber J.A. & Gates D.M. (1990) Gas exhange in *Quercus rubra* (northern red oak) during a drought: analysis of relations among photosynthesis, transpiration, and leaf conductance. *Tree Physiology* **7,** 215–225.

Whitehead D. & Hinckley T.M. (1991) Models of water flux through forest stands: Critical leaf and stand parameters. *Tree Physiology* **9,** 35–57.

Wofsy S.C., Goulden M.L., Munger J.W. Fan, S.-M., Bakwin P.S., Daube B.C., Bassow S.L. & Bazzaz F.A. (1993) Net exchange of CO_2 in a mid-latitude forest. *Science* **260,** 1314–1317.

Wullschleger S.D. (1993) Biochemical limitations to carbon assimilation in C_3 plants -a retrospective analysis of the A/C_i curves from 109 species. *Journal of Experimental Botany* **44,** 907–920.

Yoder B.J., Ryan M.G. & Kaufmann M.R. (1994) Evidence of reduced photosynthetic rates in old trees. *Forest Science* **40,** 513–527.

Received 10 October 1995; received in revised form 30 January 1996; accepted for publication 19 February 1996

APPENDIX

The canopy foliar N distribution (g N m^{-2} leaf area, in layer n) is given by

$$N_n = N\, n_{top} \exp[n_{sl}(n-1)], \tag{A1}$$

and the soil hydraulic resistance to canopy layer n (R_{sn}; MPa s m^2 $mmol^{-1}$) by

$$R_{sn} = \frac{\ln(r_s/r_s)}{2\pi l_r L_{soil}}. \tag{A2}$$

The canopy layer hydraulic resistance (R_{pn}; MPa s m^2 $mmol^{-1}$), which includes root, stem and branch resistance, is given by

$$R_{pn} = \frac{h}{G_p}, \tag{A2}$$

and the canopy layer capacitance (C_n, mmol MPa^{-1} m^{-2})by

$$C_n = \frac{dW_n}{d\Psi_{ln}}. \tag{A4}$$

The steady-state water flux through a canopy layer (J_n; mmol m^{-2} s^{-1}) can be written

$$J_n = (\Psi_s - \Psi_{ln} - \rho_w g h)/(R_{sn} + R_{pn}). \tag{A5}$$

The rate of change of layer water content (dW_n/dt) is given by the difference between the flow of water into the layer and that lost by transpiration from that layer:

$$dW_n/dt = J_n - E_n. \tag{A6}$$

Thus,

$$dW_n/dt = (\Psi_s - \Psi_{ln} - \rho_w g h)/(R_{sn} + R_{pn}) - E_n. \tag{A7}$$

Substitution of Eqn A4 into EqnA7 gives

$$\Delta\Psi_{ln} = \Delta t\, \frac{\Psi_s - \rho_w g h - E_n(R_{sn} + R_{pn}) - \Psi_{ln}}{C_n(R_{sn} + R_{pn})}. \tag{A8}$$

The new $\Psi_{ln(t+1)}$ is simply determined by

$$\Psi_{ln(t+1)} = \Psi_{ln} + \Delta\Psi_{ln}. \tag{A9}$$

The CO_2 diffusion model, calculated separately for each layer (Von Caemmerer & Farquhar 1981), is

$$A = (g_t - 0{\cdot}5E)C_a - (g_t + 0{\cdot}5E)C_i. \tag{A10}$$

The total CO_2 conductance from atmosphere to mesophyll (g_t; mol m^{-2} s^{-1}) is given by

$$g_t = \frac{P/RT_l}{1{\cdot}65/g_s + 1{\cdot}37/g_b + 1/g_i}. \tag{A11}$$